Progress In Electromagnetics Research M, Vol. 56, 81–90, 2017

Rough Surface Scattering via Two-Way Parabolic Integral Equation

Mark Spivack* **and Orsola Rath Spivack**

Abstract—This paper extends the parabolic integral equation method, which is very effective for forward scattering from one-dimensional rough surfaces, to include backscatter. This is done by applying left-right splitting to a modified two-way governing integral operator, to express the solution as a series of Volterra operators; this series describes successively higher-order surface interactions between forward and backward going components, and allows highly efficient numerical evaluation. This and equivalent methods such as ordered multiple interactions have been developed for the full Helmholtz integral equations, but not previously applied to the parabolic Green's function. Equations are derived for both Dirichlet and Neumann boundary conditions (TE and TM).

1. INTRODUCTION

Wave scattering from irregular surfaces continues to present formidable theoretical and computational challenges [1–7], especially with regard to numerical solution for wave incidence at low grazing angles [8–13], where the illuminated region may become very large. There are many such situations including radar scattering by sea surfaces and scattering in engine ducts. Computationally, the cost of the necessary matrix inversion scales badly with wavelength and domain size and can rapidly become prohibitive; this is compounded by the large number of Green's function evaluations, whose overall cost is therefore sensitive to the form which this function takes.

Under the assumption of purely forward-scattering, a successful approach has been the parabolic integral equation method (PIE) [14–17]. This makes use of a 'one-way' parabolic equation (PE) Green's function, leading to the replacement of the Helmholtz integral equations by their small-angle analogue. For 2D problems this Green's function takes a particularly tractable form; this, together with the Volterra (one-sided) form of the governing integral operator, affords the key advantage of high numerical efficiency, and in the perturbation regime allows derivation of analytical results [13, 18–20]. There is also a growing interest in imaging and surface reconstruction, with some successes by methods tailored to the regime including back-propagation and iterative methods for high incident angles, and PE-related approaches at low angles [21–25]. Nevertheless, the PE method yields little information about the field scattered back towards the source.

On the other hand, where backscatter is required, operator series solution methods such as left-right splitting (L-R) and method of ordered multiple interactions [26–33] have proved highly versatile, in both 2 and 3 dimensions. These use the full free-space Green's function and proceed by expanding the surface fields about the dominant 'forward-going' component, and thereby circumvent the difficulties of tackling the full Helmholtz equations.

In this paper we combine these approaches, extending the standard PIE description to a 'two-way' method, thus allowing for both left- and right-travelling waves and the interaction between them. This is obtained in the obvious way by replacing the parabolic equation Green's function by a form symmetrical in range (to within a phase factor). The integral operator can be split into left- and right-going parts;

Received 18 February 2017, Accepted 12 April 2017, Scheduled 23 April 2017

* Corresponding author: Mark Spivack (ms100@cam.ac.uk).

The authors are with the Centre for Mathematical Sciences, University of Cambridge, CB3 0WA, UK.

under the assumption that forward scattering dominates, the solution can then be written as a series and truncated. Every term of this series is a product of Volterra operators and is therefore as efficient as the standard PIE method, which corresponds approximately[†] to truncation at the first term. This has a number of benefits: It provides a highly efficient computational means to include backscatter, via a relatively simple modification of existing codes; and the corresponding correction term provides useful information about the left-right interactions. With additional constraints it also gives rise to analytically tractable expressions for the higher statistical moments. We present numerical results to serve two main purposes: to compare with well-validated exact numerical calculations and with left-right splitting using the full Helmholtz equations; and to examine the effect of including leading order backscatter and its interaction with the forward-scattered field in the parabolic regime.

The paper is organised as follows: The standard parabolic integral equation method and preliminary results are given in Section 2. In Section 3 the full two-way parabolic integral equation method is set out, and the iterative solution explained. Computational results are given comparing the two-way PIE method with both the previously validated Helmholtz left-right splitting, and with exact numerical calculations.

2. PARABOLIC INTEGRAL EQUATION METHOD AND PRELIMINARIES

We consider the 2-dimensional problem of a scalar time-harmonic wave field p scattered from a perfectly conducting rough surface $h(x)$, both for transverse electric (TE) and transverse magnetic (TM) incident fields. This is equivalent to a corrugated surface in 3-D with the surface generator aligned with the plane of incidence, so that the TE and TM scattering problems a decoupled. In the description below we concentrate mainly on the TE case; expressions are also given for the TM case for which the derivation is similar. The wavefield has wavenumber k and is governed by the wave equation $(\nabla^2 + k^2)p = 0$. The coordinate axes are x and z where x is the horizontal and z is the vertical, directed out of the medium (see Fig. 1). Angles of incidence and scatter are assumed to be small with respect to the positive x-direction. It will be assumed that the surface is statistically stationary to second order, i.e., its mean and autocorrelation function are translationally invariant. We may choose coordinates so that $h(x)$ has mean zero. The autocorrelation function $< h(x)h(x+\xi) >$ is denoted by $\rho(\xi)$, and we assume that $\rho(\xi) \to 0$ at large separations ξ. (The angled brackets here denote the ensemble average.) Then $\sigma^2 \equiv \rho(0)$ is the variance of surface height, so that the surface roughness is of order $O(\sigma)$.

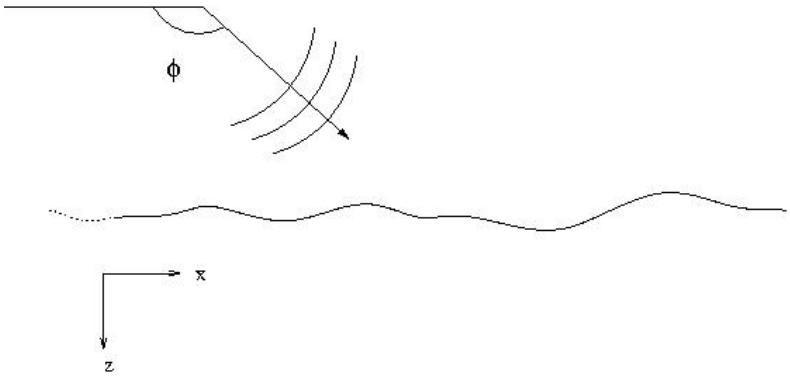

Figure 1. Schematic view of scattering geometry.

Since the field components propagate predominantly around the x-direction, we can define a slowly-varying part ψ by

$$\psi(x,z) = p(x,z)\ \exp(-ikx). \tag{1}$$

Slowly varying incident and scattered components ψ_i and ψ_s are defined similarly, so that $\psi = \psi_i + \psi_s$. It may be assumed that $\psi_i(x, h(x)) = 0$ for $x \leq 0$, so that the area of surface illumination is restricted,

[†] Note however that in contrast to standard PIE the first term includes 'direct backscatter' without additional effort.

as it would be for example in the case of a directed Gaussian beam. The governing equations for the standard parabolic equation method for TE polarized wave (Dirichlet boundary condition) [14, 15] are then

$$\psi_i(\mathbf{r}_s) = -\int_0^x G_p(\mathbf{r}_s;\mathbf{r}')\frac{\partial\psi(\mathbf{r}')}{\partial z}\,dx' \tag{2}$$

where both $\mathbf{r}_s = (x, h(x))$, $\mathbf{r}' = (x', h(x'))$ lie on the surface; and

$$\psi_s(\mathbf{r}) = \int_0^x G_p(\mathbf{r};\mathbf{r}')\frac{\partial\psi(\mathbf{r}')}{\partial z}\,dx' \tag{3}$$

where $\mathbf{r}'$ is again on the surface and $\mathbf{r}$ is an arbitrary point in the medium. Here G_p is the parabolic form of the Green's function in two dimensions given by

$$G_p(x,z;x',z')\begin{cases} = \alpha\sqrt{\dfrac{1}{x-x'}}\,\exp\Big[\dfrac{ik(z-z')^2}{2(x-x')}\Big] & \text{for } x' < x \\ = 0 & \text{otherwise} \end{cases}$$

where $\alpha = \frac{1}{2}\sqrt{i/2\pi k}$. This asymmetrical form gives rise to the finite upper limit of integration in Equations (2) and (3). It is derived under the assumption of forward-scattering, and that the field obeys the parabolic wave equation,

$$\psi_x + 2ik\psi_{zz} = 0 \tag{4}$$

which holds provided that the angles of incidence and scattering are fairly small with respect to the x-direction. (G_p can also be obtained directly from the full free space Green's function under the small-angle approximation.) Equation (2) must be inverted to give the induced source $\partial\psi/\partial z$ at the surface, which is then substituted in Equation (3) to determine the field elsewhere.

Consider an incident plane wave $p = \exp(ik[x\sin\theta + z\cos\theta])$, where θ is the angle with respect to the vertical. The grazing angle is then denoted $\mu = \pi/2 - \theta$ (see Fig. 1). This plane wave has slowly-varying component $\psi^\theta = \exp(ik[Sx + z\cos\theta])$, where

$$S = \sin\theta - 1, \tag{5}$$

which we refer to as the reduced plane wave.

3. TWO-WAY PARABOLIC INTEGRAL EQUATION METHOD

In this section the two-way version of the parabolic integral equation method will be described, and the iterative solution will be given. This provides an efficient means of including forward- and back-scattered components at small angles of scatter.

3.1. The Modified Governing Equations

The governing Equations (2), (3) must first be modified to take into account scattering from the right. To do this, we simply replace G_p by its symmetrical analogue G. This form arises if we apply the small angle approximation described in Section 2 to the full free space Green's function without requiring $G(x,z;x',z')$ to vanish when $x' \geq x$. We thus obtain

$$G(x,z;x',z')\begin{cases} = \alpha\sqrt{\dfrac{1}{|x-x'|}}\,\exp\left[\dfrac{ik(z-z')^2}{2|x-x'|}\right], & x' < x \\ = \alpha\sqrt{\dfrac{1}{|x-x'|}}\,\exp\left[\dfrac{ik(z-z')^2}{2|x-x'|}\right]\,\exp\left[2ik|x-x'|\right] & x' \geq x \end{cases} \tag{6}$$

The factor $\exp[-2ik(x'-x)]$ arises for $x' \geq x$ because we are solving for the reduced wave ψ.

Applying this Green's function to the reduced wave ψ we obtain

$$\psi_s(x,z) = \int_0^\infty G(\mathbf{r},\mathbf{r}')\frac{\partial\psi(\mathbf{r}')}{\partial z}dx'. \tag{7}$$

This is the analogue of Equation (2), effectively containing a back-scatter correction. Taking the limit of Equation (7) as $z \to h(x)$ yields an integral equation relating the incident field to the scattered field at the surface:

$$\psi_i(x, h(x)) = -\int_0^\infty G(\mathbf{r}_s, \mathbf{r}') \frac{\partial \psi(\mathbf{r}')}{\partial z} dx' \tag{8}$$

where now $\mathbf{r}_s$, $\mathbf{r}'$ both lie on the surface. (Note that the addition of a correction to the parabolic equation is closely related to a method proposed by Thorsos [14].) Equations (7), (8) can be written in operator notation:

$$\psi_s(x, z) = -(L + R)\frac{\partial \psi}{\partial z} \tag{9}$$

$$\psi_i(x, h(x)) = (L + R)\frac{\partial \psi}{\partial z} \tag{10}$$

where L, R are defined by

$$Lf(x, z) = \int_0^x G(\mathbf{r}, \mathbf{r}') f(x') dx', \qquad Rf(x, z) = \int_x^\infty G(\mathbf{r}, \mathbf{r}') f(x') dx'.$$

These integral operators and their inverses are Volterra, or 'one-sided' in an obvious sense.

3.2. Solution of the Modified Equations

The main computational task in any such boundary integral method is the inversion of the integral Equation (10). One of the principal advantages of the standard forward-going PIE method (Equations (2)–(3)) is that its one-way form allows Gaussian elimination to be used, so that inversion is highly efficient. In the above two-way formulation this advantage is initially lost, since direct inversion of $L+R$ in Equation (10) offers no benefit compared with solving the full Helmholtz equations. However, the computational advantage can be regained by forming an iterative series solution, in which each term is a product of Volterra integral operators.

Integral Equation (10) has formal solution

$$\frac{\partial \psi}{\partial z} = (L + R)^{-1} \psi_i \tag{11}$$

which can be expanded in a series

$$\frac{\partial \psi}{\partial z} = \left[L^{-1} - L^{-1} R L^{-1} + \left(L^{-1} R\right)^2 L^{-1} - \ldots \right] \psi_i \tag{12}$$

Under the assumption that R is 'small' (as is already required implicitly for the standard PIE solution) the series in Equation (12) is convergent; the series can then be truncated after finitely many terms. By 'small' we mean that $R\phi/||\phi||$ is small for all terms ϕ in the series. It can be shown that this assumption is indeed justified at low grazing angles for surfaces whose slopes are not too large, since the kernel of R oscillates rapidly especially at small wavelengths. It is nevertheless difficult to give this a precise range of validity, and we will not attempt to do so here.

Solution for the field can therefore be obtained by truncating the series in Equation (12) and substituting into the integral in Equation (7). The *first term* $L^{-1}\psi_i$ in series in Equation (12) corresponds to the solution for $\partial\psi/\partial z$ under the standard PIE method (e.g., [15]). Denote this first approximation by $\tilde{\psi}$, i.e.,

$$\frac{\partial \psi}{\partial z} \cong \tilde{\psi} = L^{-1} \psi_i. \tag{13}$$

Note however that the integral in Equation (7) using the two-way Green's function allows for outgoing components scattered to the left, unlike its PIE analogue in Equation (3), so even this lowest order truncation gives backscatter. This can be considered the *direct backscatter* component.

Truncation of Equation (12) at the *second term* gives:

$$\frac{\partial \psi}{\partial z} \cong \tilde{\psi} + C \tag{14}$$

where C is a correction term,

$$C = -L^{-1}RL^{-1}\psi_i. \tag{15}$$

We remark that this is the lowest-order truncation consistent with reversible ray paths.

3.3. Numerical Evaluation

The general term of Equation (12) is a product of the operators L^{-1} and R. Evaluation of the integral R is straightforward. For computational purposes we assume that the incident wave illuminates only a finite region of the rough surface; the source may for example be a Gaussian beam. A finite upper limit of integration $x_{\max}$, say, may then be assumed.

Numerical inversion of L is also highly efficient since discretization of L gives rise to a lower-triangular matrix. This has been described elsewhere (e.g., [15]) and will only be summarized here.

Consider the equation $L\partial\psi/\partial z = \psi_i$ obtained by truncating Equation (12) at the first term. This equation is discretized with respect to range x using, say, N equally spaced points x_j. This then yields a matrix equation $A\partial\psi/\partial z = \psi_i$ in which the matrix A is lower-triangular. Numerical inversion of this expression is carried out by Gaussian elimination, requiring $O(N^2)$ operations, which compares with $O(N^3)$ operations required to treat the full Helmholtz integral equation. An important additional advantage in 2-dimensional problems is that the Green's function is in closed form and much quicker to evaluate, than the Hankel functions which can be a major component of computational expense for the full Helmholtz Green's function. (This situation is reversed, however, when moving to 3-dimensional scattering.)

The solution is thereby obtained for the first term, $\tilde{\psi}$. Typically only one further term, $L^{-1}R\tilde{\psi}$, will be required. The simplest way to obtain this is to discretize the integral R, evaluate $R\tilde{\psi}$ numerically, and then to solve

$$L^{-1}R\tilde{\psi} = \frac{\partial\psi}{\partial z} - \tilde{\psi}$$

by Gaussian elimination as before. The evaluation of the integral R also requires $O(N^2)$ operations. Subsequent terms in the series may be obtained similarly.

The computation can be simplified further in the perturbation regime of small scaled surface height $k\sigma$, if the operators L and R are replaced by the flat surface forms in the calculation of the correction term C. This will be discussed in a separate paper.

3.4. Computational Examples

We now present some results for both TE and TM in order to illustrate the method, focusing on the surface fields. We compared the parabolic equation (PIE) results with both Helmholtz L-R splitting and the BAE data published in [29]. All parameters are chosen as in that reference to provide a consistent basis for comparison. We also use the same rough surface profiles with Gaussian and power law autocorrelation functions as in that reference, shown in Fig. 2. For the purpose of these calculations the rough surface was embedded in a longer section of flat surface, part of which can be seen in here. The total number of surface grid points was around 8×10^3 (in order to solve for around 4×10^3 unknowns). The rough part of the surfaces was around 10 λ where λ denotes the wavelength. The frequency of the incident field was 10 GHz, so that $\lambda = 0.03$ m. Peak-to-trough heights were around 4 mm for the TM calculations and 20 mm for TE. In both cases the solutions represent surface currents $\mathbf{J}(x)$. The incident field was taken to be a plane wave at a grazing angle of 10°, tapered at the edges of the domain to minimize spurious edge effects. (This tapering is not crucial as the rough surface patch is many wavelengths from the edges of the extended domain.) The time taken in each of these examples was of the order of a few seconds or less on a standard Linux workstation (Intel i5-6500 3.2 GHz processor). The BAE 'exact' results were generated using 2D finite element time domain software (more details for which are given in [29]).

In most cases the PIE results at each iteration may be expected to be less accurate than those of Helmholtz L-R splitting. Nevertheless close agreement is seem with L-R splitting at each iteration, and even at the first iteration good correspondence is found when comparing with exact solutions.

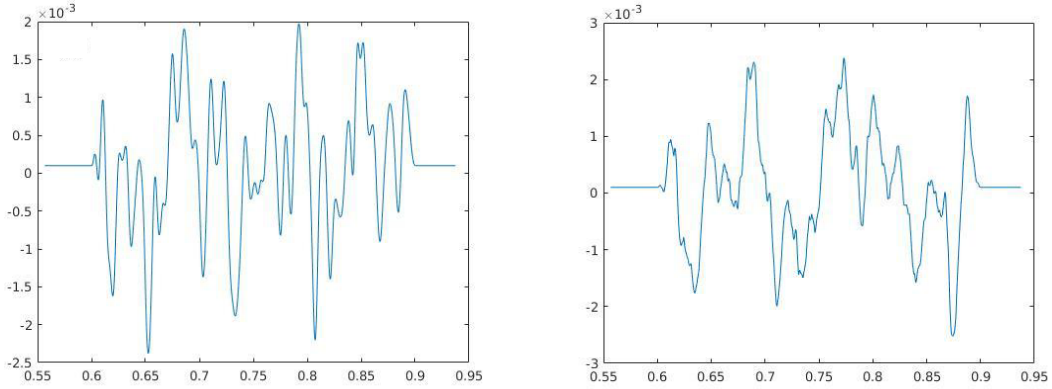

Figure 2. Surfaces with (a) Gaussian autocorrelation function and (b) power law autocorrelation function as used in these computations.

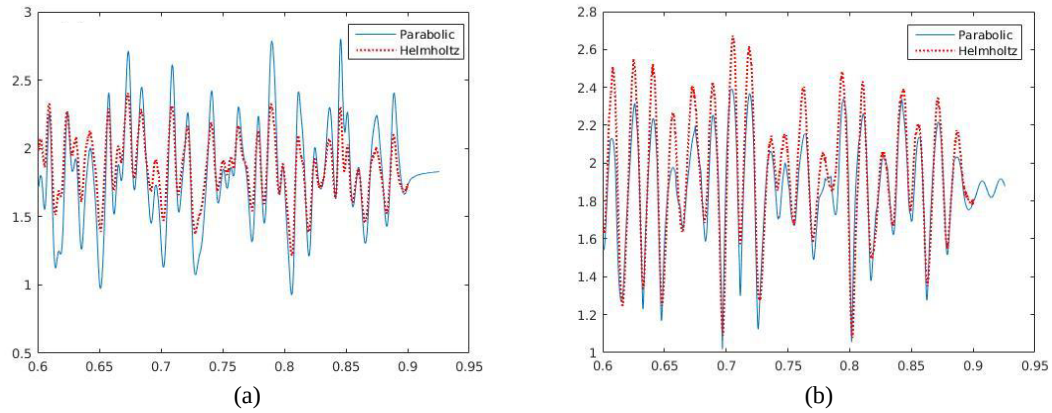

Figure 3. Comparison between parabolic integral equation (—) and Helmholtz left-right splitting (. . .) (a) first iteration and (b) second iteration for the Gaussian surface of Fig. 2(a).

Fig. 3 compares PIE and Helmholtz L-R splitting for (a) the first and (b) the second iterations, for the Gaussian surface, for TM polarised wave.

It can be noticed that the more accurate second iterations appear somewhat more regular; this is due to an interference effect between left- and right-going components which is absent at the first iteration. Fig. 4 shows an expanded region of the parabolic equation solution at first and second iterations in order, demonstrating the effect of backscatter which the two-way formulation allows to be taken into account.

PIE and Helmholtz L-R results were then compared at the first two iteration for the more 'jagged' power law surface. Results corresponding to those of Fig. 3 are shown in Fig. 5, and again show good agreement.

ure

The PIE results at the second iteration were also compared directly with the BAE computations, as shown in Fig. 6. Somewhat surprisingly these appear better than those of the Helmholtz L-R calculation. This should, however, be viewed with caution. The key difference is that the Helmholtz results for the power law surface exhibit an unexpected sensitivity to the sharper small scale surface features. This is likely to be an artifact of numerical implementation rather than a fundamental property of the approximations.

Finally in Fig. 7 we show an example of the first iteration of the PIE solution for TE polarized incident field, corresponding again to the parameters used in [29]. The surface corresponds to Fig. 2(a)

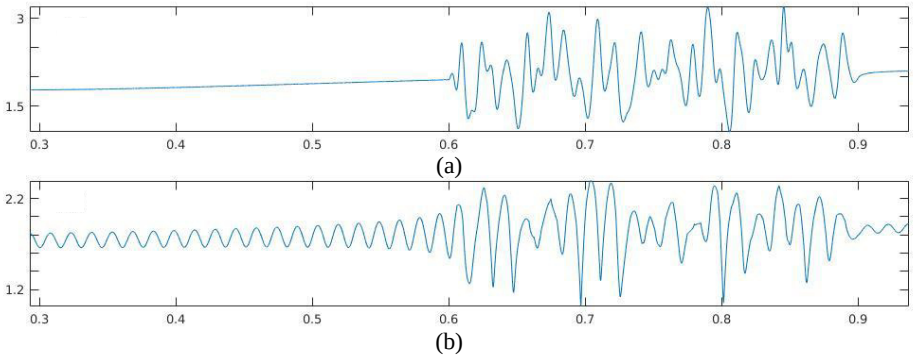

Figure 4. Result from (a) first iteration and (b) second iteration, illustrating backscatter component due to two-way Green's function.

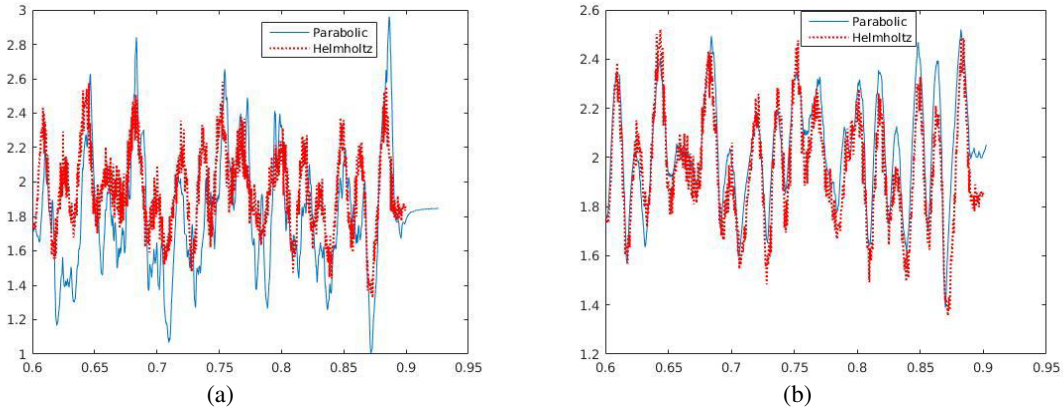

Figure 5. Comparison between parabolic integral equation (—) and Helmholtz left-right splitting (...) (a) first iteration and (b) second iteration for the power-law surface of Fig. 2(b).

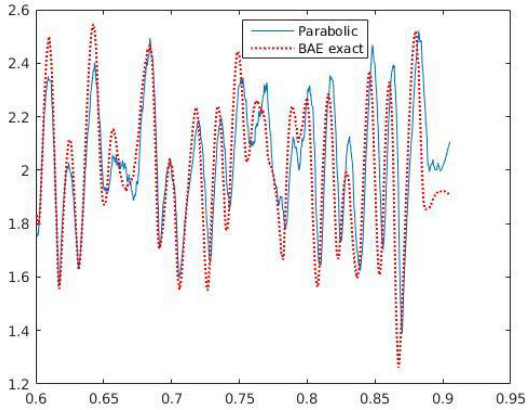

Figure 6. Comparison between second iteration of parabolic integral equation (—) and exact results (...) for power-law surface Fig. 2(b).

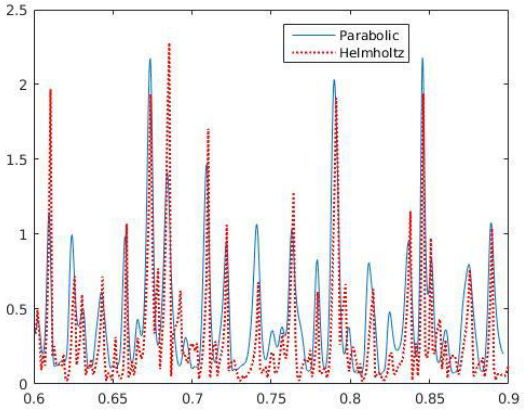

Figure 7. Comparison between parabolic integral equation and Helmholtz left-right splitting at the first iteration, for TE case.

scaled up by a factor of 5. Again this shows fairly good agreement. However, for this boundary condition the second iteration (not shown) is less satisfactory.

Regarding the limits of accuracy and the convergence of this approach, we note that he surface heights in the benchmark data for this comparison were fairly small. However, the (one-way) parabolic equation has been shown to be stable and valid for surface heights which can be very much greater than a wavelength provided scattering angles remain fairly small, which equates to moderate surface slopes. Rates of convergence of the iterative 'left-right' series also depend principally on scattering angles, both for the parabolic and full Green's functions, and in both 2- or 3-dimensions. The parabolic regime therefore lends itself to rapid convergence of the left-right series and when the parabolic equation is accurate we can expect good convergence. However, the converse is not true, i.e., convergence does not guarantee accuracy.

4. CONCLUSIONS

The parabolic integral equation method has been extended here to allow the calculation of backscatter due to a scalar wave impinging on a rough surface at low grazing angles. The solution is written in terms of a series of Volterra operators, each of which is easily evaluated, and which allows examination of multiple scattering resulting from increasing orders of surface interaction. Truncation at the first term yields the leading forward- and back-scattered components; higher-order multiple scattering are available from subsequent terms and have been calculated here. Comparisons have been presented with validated results from the operator series solution using the full Green's function and exact numerical solutions, for specific well-characterised surfaces. The parabolic Green's function is applicable for wave components at low angles of incidence and scatter, which imply small surface slopes, but without restriction on surface heights.

With the additional assumption of small surface heights, analytical solutions may be obtained to second order in height for the mean field and its autocorrelation. These provide backscatter corrections to the solutions given in the purely forward-scattered case [18, 19] with the potential for further insight into the role of different orders of multiple scattering. This is the subject of a separate paper.

In the context of long-range propagation at low grazing angles, parabolic equation methods remain very widely used both in 2- and 3-dimensional settings. In this regime the form of the Green's function together with the series decomposition provide computational efficiency and the means to extend existing PE methods to include backscatter, in addition to yielding tractable analytical results for statistical moments. These benefits should, nevertheless, be put in context. One-dimensional surface models are frequently used and often directly applicable in narrow angle propagation as well as for corrugated surfaces and inverse problems, but the aim should most often be methods which give theoretical insight or allow computation for the general scattering problem. In particular there remains a need for further theoretical understanding of the mechanisms of enhanced and multiple backscatter. Several computational advantages of the parabolic Green's function (such as its closed form) are lost in full 3-dimensional problems, or those for which wide-angle scatter needs to be taken into account. On the other hand the approach here may be applied in the more general setting, with the PE Green's function replaced by the full 3D Green's function which is relatively tractable. Computationally that method has already proved successful [32]. However, in the interaction between forward- and back-scattered fields in 3D has not yet been examined, and analytical treatment of the 3D statistics via this approach remains a challenge.

ACKNOWLEDGMENT

The authors are grateful to Jill Ogilvy and Colin Sillence for numerous discussions and crucial insights. The first author is also grateful to BAE Systems for data and financial support during formative stages of the work. The authors also thank anonymous referees for helpful suggestions and corrections.

APPENDIX A. EQUATIONS FOR TM POLARIZED FIELD

For a TM polarized incident field (Neumann boundary conditions) the governing equations for the one-way parabolic integral equation have been given elsewhere [17]. The extension to the two-way parabolic integral equation is exactly analogous to the formulation for the TE case.

We require the derivative $H = \partial G/\partial z'$ of G with respect to the second vertical coordinate:

$$H_p(x,z;x',z') \begin{cases} = \alpha \dfrac{z-z'}{|x-x'|^{3/2}} \exp\left[\dfrac{ik(z-z')^2}{2|x-x'|}\right], & x' < x \\ = \alpha \dfrac{z-z'}{|x-x'|^{3/2}} \exp\left[\dfrac{ik(z-z')^2}{2|x-x'|}\right] \exp\left[2ik|x-x'|\right] & x' \geq x \end{cases} \tag{A1}$$

The factor $\exp[-2ik(x'-x)]$ again arises for $x' \geq x$ because we are solving for the reduced wave ψ. The governing integral equations are similar to Equations (7) and (8) although care is needed in interpreting the integrals because of the singularity in the Green's function as its arguments coalesce:

$$\psi_i(\mathbf{r}_s) = \frac{\psi(\mathbf{r})}{2} + \int_0^\infty H_p(\mathbf{r}_s;\mathbf{r}')\psi(\mathbf{r}')\, dx' \tag{A2}$$

where both $\mathbf{r}_s = (x, h(x))$, $\mathbf{r}' = (x', h(x'))$ lie on the surface; and

$$\psi_s(\mathbf{r}) = -\int_0^\infty H_p(\mathbf{r};\mathbf{r}')\psi(\mathbf{r}')\, dx' \tag{A3}$$

where $\mathbf{r}'$ is again on the surface and $\mathbf{r}$ is an arbitrary point in the medium. This can again be written in terms of left- and right-going operators L and R, and the iterative series solution for this is exactly analogous to Equations (11) and (12) for the TE case.

REFERENCES

1. Warnick, K. F. and W. C. Chew, Numerical methods for rough surface scattering, *Waves in Random Media*, Vol. 11, R1–R30, 2001.
2. Zhang, B. and S. N. Chandler-Wilde, "Integral equation methods for scattering by infinite rough surfaces," *Math. Meth. in Appl. Sci.*, Vol. 26, 463–488, 2003.
3. Ogilvy, J. A., *The Theory of Wave Scattering from Random Rough Surfaces*, IOP Publishing, Bristol, 1991.
4. DeSanto, J. A. and G. S. Brown, "Analytical techniques for multiple scattering," *Progress in Optics*, Vol. 23, ed. E. Wolf, Elsevier, New York, 1986.
5. Voronovitch, A. G., *Wave Scattering from Rough Surfaces*, 2nd Edition, Springer Science and Business Media, Berlin, 2013.
6. Saillard, M. and A. Sentenac, "Rigorous solutions for electromagnetic scattering from rough surfaces," *Waves in Random Media*, Vol. 11, R103–R137, 2001.
7. Simonsen, I., A. A. Maradudin, and T. A. Leskova, "Scattering of electromagnetic waves from two-dimensional randomly rough perfectly conducting surfaces: The full angular intensity distribution," *Physical Review A*, Vol. 81 013806, 1–13, 2010.
8. Chan, H. C., "Radar sea clutter at low grazing angles," *IEE Proc. Radar Signal Processing*, F 137, 102–112, 1990.
9. Watson, J. G. and J. B. Keller, "Rough surface scattering via the smoothing method," *J. Acoust. Soc. Am.*, Vol. 75, 1705–1708, 1984.
10. Bruce, N. C., V. Ruizcortes, and J. C. Dainty, "Calculations of grazing incidence scattering from rough surfaces using the Kirchhoff approximation," *Opt. Comm.*, Vol. 106, 123–126, 1994.
11. Sum, K. S. and J. Pan, "Scattering of longitudinal waves, (sound) by defects in fluids. Rough surface *J. Acoust. Soc. Am.*, Vol. 122, 333–344, 2007.

12. Qi, C., Z. Zhao, W. Yang, Z. P. Nie, and G. Chen, "Electromagnetic scattering and Doppler analysis of three-dimensional breaking wave crests at low-grazing angles," *Progress In Electromagnetics Research*, Vol. 119, 239–252, 2011.
13. Janaswamy, R., "Direct solution of current density induced on a rough surface by forward propagating waves," *IEEE Transactions on Antennas and Propagation*, Vol. 61, 3728–3738, 2013.
14. Thorsos, E., "Rough surface scattering using the parabolic wave equation," *J. Acoust. Soc. Am.*, Suppl. 1, Vol. 82, S103, 1987.
15. Spivack, M., "A numerical approach to rough surface scattering by the parabolic equation method," *J. Acoust. Soc. Am.*, Vol. 87, 1999–2004, 1990.
16. Tappert, F. and L. Nghiem-Phu, "A new split-step Fourier algorithm," *J. Acoust. Soc. Am.*, Suppl. 1, Vol. 77, S101, 1987.
17. Spivack, M. and B. J. Uscinski, "Numerical solution of scattering from a hard surface in a medium with a linear profile," *J. Acoust. Soc. Am.*, Vol. 93, 249–254, 1993.
18. Spivack, M., "Coherent field and specular reflection at grazing incidence on a rough surface," *J. Acoust. Soc. Am.*, Vol. 95, 694–700, 1994.
19. Spivack, M., "Moments and angular spectrum for rough surface scattering at grazing incidence," *J. Acoust. Soc. Am.*, Vol. 97, 745–753, 1995.
20. Uscinski, B. J. and C. J. Stanek, "Acoustic scattering from a rough sea surface: the mean field by the integral equation method," *Waves in Random Media*, Vol. 12, 247–263, 2002.
21. Bao, G. and L. Zhang, "Shape reconstruction of the multi-scale rough surface from multi-frequency phaseless data," *Inverse Problems*, Vol. 32 1–16, 2016.
22. "Reconstruction of a heterogeneous fractal surface profile from scattering measurements at low grazing incidence," *Antennas and Propagation Society International Symposium, 2005 IEEE*, Vol. 3, 445–448, 2005.
23. Spivack, M., "Solution of the inverse scattering problem for grazing incidence upon a rough surface," *J. Opt. Soc. A*, Vol. 9, 1352–1355, 1992.
24. Cai, Z., D. Chen, and S. Lu, "Reconstruction of a fractal rough surface," *Physica D: Nonlinear Phenomena*, Vol. 213, 25–30, 2006.
25. Akduman, I., R. Kress, and A. Yapar, "Iterative reconstruction of dielectric rough surface profiles at fixed frequency," *Inverse Problems*, Vol. 22, 939, 2006.
26. Kapp, D. A. and G. S. Brown, "A new numerical method for rough surface scattering calculations," *IEEE Trans. Ant. Prop.*, Vol. 44, 711–721, 1996.
27. Zhang, X., Z. Wu, T. Wu, and Y. Wei, "A study of electromagnetic scattering from sea surface with breaking waves using generalized forward-backward method," *Ant. Prop. and EM Theory, ISAPE), 2016 11th International Symposium, IEEE*, 472–474, 2016.
28. Spivack, M., "Forward and inverse scattering from rough surfaces at low grazing incidence," *J. Acoust. Soc. Am.*, Vol. 95, Pt 2, 3019, 1994.
29. Spivack, M., A. Keen, J. Ogilvy, and C. Sillence, "Validation of left-right method for scattering by a rough surface," *J Modern Optics*, Vol. 48 1021–1033, 2001.
30. Tran, P., "Calculation of the scattering of electromagnetic waves from a two-dimensional perfectly conducting surface using the method of ordered multiple interaction," *Waves in Random Media*, Vol. 7, 295–302, 1997.
31. Adams, R. J., "Combined field integral equation formulations for electromagnetic scattering from convex geometries," *IEEE Trans. Ant. Prop.*, Vol. 52, 1294–1303, 2004.
32. Spivack, M., J. Ogilvy, and C. Sillence, "Electromagnetic scattering by large complex scatterers in 3D," *IEE Proc Science, Measurement and Tech.*, Vol. 151 464–466, 2004.
33. Pino, M. R., L. Landesa, J. L. Rodriguez, F. Obelleiro, and R. J. Burkholder, "The generalized forward-backward method for analyzing the scattering from targets on ocean-like rough surfaces," *IEEE Trans. Ant. Prop.*, Vol. 47, 961–969, 1999.